GEORGIA INSTITUTE OF TECHNOLOGY OFFICE OF CONTRACT ADMINISTRATION

PROJECT ADMINISTRATION DATA SHEET

[x] ORIGINAL [ ] REVISION NO. _____

Project No. A-3045 DATE 9/15/81

Project Director: C. H. Cash ~~School~~ Lab RAIL/OOD

Sponsor: U. S. Army Missile Command; Redstone Arsenal, AL 35898

Type Agreement: Delivery Order No. 0028 under Contract No. DAAH01-81-D-A003

Award Period: From 8/27/81 To 12/31/81 (Performance) 2/10/82 (Reports)

Sponsor Amount: $50,000 Contracted through:

Cost Sharing: None GTRI/~~GIT~~

Title: Helicopter Mast Mounted Sensor Analysis

ADMINISTRATIVE DATA OCA Contact William F. Brown x4820

1) Sponsor Technical Contact:

Dr. M. M. Hallum
Systems Simulation and Development Directorate
U. S. Army Missile Command
Attn: DRSMI-RDF
Redstone Arsenal, AL 35898
205-876-4141

2) Sponsor Admin/Contractual Matters:

Mr. Thomas A. Bryant
ONR Resident Representative
Georgia Institute of Technology
206 O'Keefe Building
Atlanta, GA 30332

Defense Priority Rating: DO-A2 under DMS Reg. 1 Security Classification: Unclassified

RESTRICTIONS

See Attached Government Supplemental Information Sheet for Additional Requirements.

Travel: Foreign travel must have prior approval – Contact OCA in each case. Domestic travel requires sponsor approval where total will exceed greater of $500 or 125% of approved proposal budget category.

Equipment: Title vests with Government; except that items costing less than $1,000 vests with GIT if prior approval to purchase is obtained from the Contracting Officer.

COMMENTS:

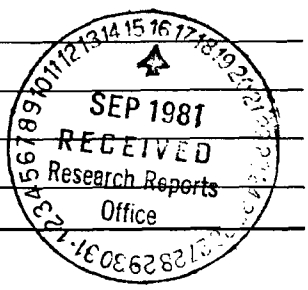

COPIES TO:

Administrative Coordinator
Research Property Management
Accounting
Procurement/EES Supply Services
Research Security Services
~~Reports Coordinator~~ (OCA)
Legal Services (OCA)
Library
EES Public Relations (2)
Computer Input
Project File
Other _____

FORM OCA 4-79A

GEORGIA INSTITUTE OF TECHNOLOGY OFFICE OF CONTRACT ADMINISTRATION

SPONSORED PROJECT TERMINATION SHEET

Date 6/9/82

Project Title: Helicopter Mast Mounted Sensor Analysis

Project No: A-3045 (D.O. #0028 under DAAH01-81-D-A003) Un. No. 51

Project Director: C. H. Cash

Sponsor: US Army Missile Command, Redstone Arsenal, AL 35898

Effective Termination Date: 12/31/81

Clearance of Accounting Charges: 2 /10/82

Grant/Contract Closeout Actions Remaining:

- ☐ Final Invoice and Closing Documents
- ☐ Final Fiscal Report
- ☐ Final Report of Inventions
- ☒ Govt. Property Inventory & Related Certificate
- ☐ Classified Material Certificate
- ☐ Other _____

Assigned to: RAIL ~~(School~~/Laboratory)

COPIES TO:

Administrative Coordinator	Research Security Services	EES Public Relations (2)
Research Property Management	~~Reports Coordinator~~ (OCA)	Computer Input
Accounting	Legal Services (OCA)	Project File
Procurement/EES Supply Services	Library	Other _____

FORM OCA 10:781

Georgia Institute of Technology
ENGINEERING EXPERIMENT STATION
ATLANTA, GEORGIA 30332

October 20, 1981

U.S. Army Missile Command
Advanced Sensors Directorate
Redstone Arsenal, Alabama 35809

Attention: Mr. John Hatcher

Subject: Monthly Progress Letter and Cost Report No. 1, Contract No. DAAH01-81-D-A003 (GIT Project A-3045) entitled "Helicopter Mast Mounted Sensor Analysis." Covering the period 17 September 1981 through 17 October 1981.

Gentlemen:

During this reporting period activities were conducted in the following areas.

1. A project work plan was prepared and team members assigned to the program.
2. Initiated sensor characterization and threat scenario definition.
3. Initiated threat and environment effects analysis.
4. Initiated study of test data and performance analysis.

COST REPORT

Project Duration:	5 Months
Months into Project:	1 Month
Funds Contracted:	$50,000.000
Funds Expended:	$ 5,154.97
Funds Remaining:	$44,845.03

Respectfully submitted,

[redacted]

Carlton H. Cash, Project Director

saw

APPROVED: [redacted]

Jerry L. Eaves, Associate Director
Radar & Instrumentation Laboratory

Georgia Institute of Technology
ENGINEERING EXPERIMENT STATION
ATLANTA, GEORGIA 30332

November 20, 1981

U.S. Army Missile Command
Advanced Sensors Directorate
Redstone Arsenal, Alabama 35809

Attention: Mr. John Hatcher

Subject: Monthly Progress Letter and Cost Report No. 2, Contract No. DAAH01-81-D-A003 (GIT Project A-3045) entitled "Helicopter Mast Mounted Sensor Analysis." Covering the period 17 October 1981 through 17 November 1981.

Gentlemen:

During this reporting period activities were conducted in the following areas:

1. Discussions were held with Litton, Loral, NRL, and MICOM personnel.

2. Analysis of the effects of multipath and rotor blades on angle accuracy and multipath elimination algorithms is underway.

3. Analysis of the effects of multiple emitters on the target sorting and location time is underway.

4. Analysis of the effects of antenna configuration and angle measurement accuracy is underway.

5. Analysis of the detection ranges against various emitters and system dynamic range requirements is underway.

COST REPORT

Project Durations:	5 Months
Months into Project:	2 Months
Funds Contracted:	$50,000
Funds Expended:	$14,552 (1 Nov. 1981)
Funds Remaining:	$28,813

Respectfully submitted,

[redacted]

Carlton H. Cash, Project Director

saw

APPROVED: [redacted]

Jerry L. Eaves, Associate Director
Radar & Instrumentation Laboratory

Final Technical Report

HELICOPTER MAST MOUNTED SENSOR ANALYSIS

by

George W. Ewell, Neal T. Alexander, Carlton H. Cash,
Stephen P. Zehner, and James S. Ussailis

Prepared for

U.S. Army Missile Command
DRSMI-IYE/Army Missile Lab
Redstone Arsenal, AL 35898

Under
Contract DAAH01-81-D-A003
Delivery Order No. 0028

Prepared by

Georgia Institute of Technology
Engineering Experiment Station
Atlanta, Georgia 30332

February 1982

REPORT DOCUMENTATION PAGE

READ INSTRUCTIONS BEFORE COMPLETING FORM

1. REPORT NUMBER

2. GOVT ACCESSION NO.

3. RECIPIENT'S CATALOG NUMBER

4. TITLE (and Subtitle)
Helicopter Mast Mounted Sensor Analysis

5. TYPE OF REPORT & PERIOD COVERED
Final Technical
August 1981 - February 1982

6. PERFORMING ORG. REPORT NUMBER
A-3045-F

7. AUTHOR(s) George W. Ewell, Neal T. Alexander, Carlton H. Cash, Stephen P. Zehner, and James S. Ussailis

8. CONTRACT OR GRANT NUMBER(s)
DAAH01-81-D-A003/0028

9. PERFORMING ORGANIZATION NAME AND ADDRESS
Georgia Institute of Technology
Engineering Experiment Station
Atlanta, Georgia 30332

10. PROGRAM ELEMENT, PROJECT, TASK AREA & WORK UNIT NUMBERS

11. CONTROLLING OFFICE NAME AND ADDRESS
U.S. Army Missile Command
DRSMI-IYE/Army Missile Lab
Redstone Arsenal, AL 35898

12. REPORT DATE
February 1982

13. NUMBER OF PAGES
16

14. MONITORING AGENCY NAME & ADDRESS(if different from Controlling Office)

15. SECURITY CLASS. (of this report)
UNCLASSIFIED

15a. DECLASSIFICATION/DOWNGRADING SCHEDULE

16. DISTRIBUTION STATEMENT (of this Report)

17. DISTRIBUTION STATEMENT (of the abstract entered in Block 20, if different from Report)

18. SUPPLEMENTARY NOTES
Georgia Tech Project A-3045-000

19. KEY WORDS (Continue on reverse side if necessary and identify by block number)
Direction Finding
Mast Mounted Sight
Radio Frequency Interferometer
Time Line Analysis

20. ABSTRACT (Continue on reverse side if necessary and identify by block number)
An analysis was undertaken to determine the capabilities of an RF Interferometer (RFI) direction-finding sensor mounted on a mast above the blades of a helicopter. Available experimental test data on such sensors are limited due to the unavailability of a dense radar environment and radar varieties during the tests. Therefore, an extrapolation from the available test results to a realistic battlefield environment including expected emitter deployments and variation of sensor parameters is needed. In an attempt to perform such

TABLE OF CONTENTS

SECTION 1
INTRODUCTION

The objective of the analysis was to determine the capabilities of an RF Interferometer (RFI) direction finding (DF) sensor mounted on a mast above the blades of a helicopter. Limited experimental tests of selected RFI sensors have been conducted against available targets; the results of these tests are presented in a MICOM report by Hatcher and Dobbs. These experiments were limited due to the unavailability of a dense radar environment and radar varieties during the tests. In order to assess the performance of the sensors in a realistic battlefield environment, Georgia Tech conducted an analysis to extrapolate the test results to include multiple emitters and variation of the sensor parameters.

The general approach was as follows:

- o Collect and analyze contractor system configuration data.
- o Define a generic DF system.
- o Identify primary error sources.
- o Quantify error magnitudes (and decorrelation times).
- o Formulate time-line equations.
- o Quantify processing effects on time lines.

The analysis was limited in scope due to the lack of data in several areas. In particular, there is little available information on the magnitude and statistical characteristics of either bistatic multipath or rotor blade modulation. Both of these error sources can have a pronounced effect on system performance. In addition, because of the fluid nature of the helicopter attack scenario, the total radiation environment is not well defined in terms of the specific number and location of radar emitters. This environment should be quantified and a prioritization scheme should be developed so that a more detailed analysis can be performed. For future, more sophisticated analyses, it would also be advantageous to develop computer models of the sensor and environment so that specific sensor configurations could be evaluated and compared. The analysis described herein was based on a generic

RFI system, so the analysis results are not dependent on a specific sensor configuration.

The effects of the scenario on the analysis include the following:

- High effective radiated power (ERP) in the main beam affects the dynamic range requirement.
- High ERP emitters can produce spurious responses due to generation of harmonics.
- CW emitters can produce spurious responses due to intermodulation with pulse signals.
- High threat density (including high-power, long-range emitters) will require prioritization to reduce processing load.
- Range measurement (via triangulation) requires an accurate DF fix from multiple locations.
- Total time line is a strong function of the multipath decorrelation time.

SECTION 2
RF INTERFEROMETER

The RF interferometer consists of two or more antenna elements spaced along a line. The amplitude and phase of the output from these elements is a function of the off-boresight angle of signals received from a radiating source and the element spacing, D, as shown for the two-element interferometer of Figure 1. The normalized output of the interferometer is

$$E(\theta) = 1 - e^{-j\phi}, \tag{1}$$

where the phase angle, ϕ, is a function of the element spacing, D, and the plane-wave incidence angle, θ, as given by

$$\phi = \frac{2\pi D}{\lambda} \sin \theta. \tag{2}$$

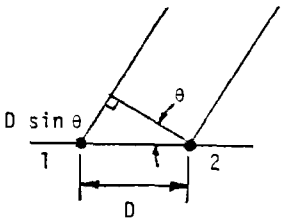

Figure 1. Two-element interferometer.

Nulls in the pattern occur when

$$\frac{2\pi D}{\lambda} \sin \theta = \pm N(2\pi) \tag{3}$$

or, conversely, when

$$\theta = \pm \sin^{-1} \left(\frac{N\lambda}{D}\right) \tag{4}$$

The electrical phase angle and resulting spatial amplitude pattern for such a two-element interferometer are shown in Figure 2. The spatial angle, θ, is unambiguous over the angular region of width θ_u, where

$$\theta_u = 2 \sin^{-1} \left(\frac{\lambda}{2D}\right). \tag{5}$$

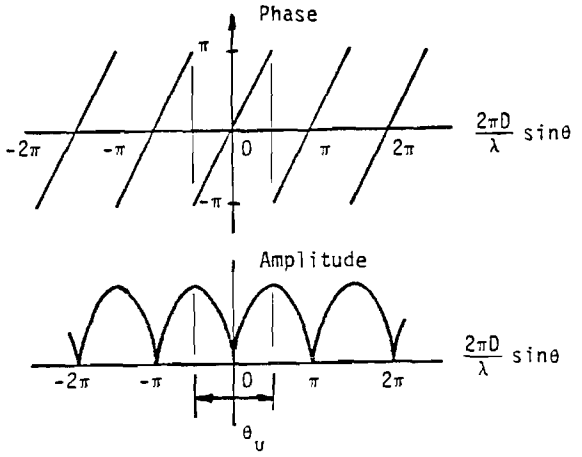

Figure 2. Interferometer patterns.

The unambiguous region for typical values of D/λ is relatively narrow, as shown below.

D/λ	θ_u
2	29.0°
5	11.5°
10	5.7°

The relationship between electrical phase angle errors in the interferometer ,$\Delta\phi$, and spatial angle errors at the interferometer output ,$\Delta\theta$, may be derived by simple differentiation. At boresight, the relationship is

$$\Delta\theta = \frac{\Delta\phi}{2\pi(D/\lambda)}. \tag{6}$$

The spatial error, $\Delta\theta$, is plotted in Figure 3 as a function of interferometer element spacing for several values of electrical phase error. At X-band, for example, for an interferometer element spacing of 12 inches ($D/\lambda = 10$) and a 5° phase error, the resulting spatial error will be less than 0.1°.

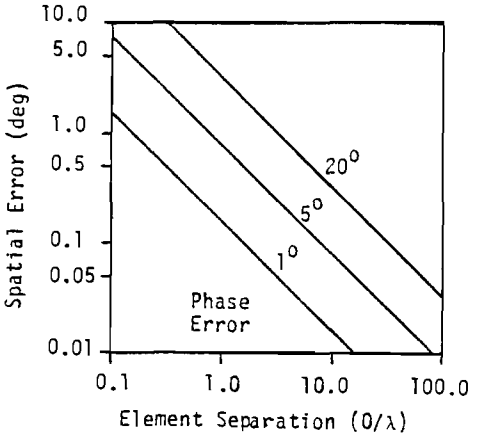

Figure 3. Interferometer spatial error.

It can be seen from the foregoing results that (1) the desire for small angular errors requires a large element spacing, while (2) the need for a large target field of view (FOV) requires a small element spacing. These conflicting requirements can be resolved by the use of additional elements at different spacings. The difference in phase between the output signals of two interferometers with spacings D_1 and D_2 is given by

$$\Delta\phi = \phi_1 - \phi_2 = \frac{2\pi\,(D_1 - D_2)}{\lambda} \sin\theta. \tag{7}$$

The unambiguous field-of-view (FOV) is now a function of the phase difference, $\Delta\phi$, and is given by

$$\text{FOV} = 2\,\sin^{-1}\,[\lambda/(D_1 - D_2)]. \tag{8}$$

SECTION 3
RECEIVER ASSESSMENT

The principal factors which determine receiver suitability are (1) dynamic range, and (2) spurious responses due primarily to intermodulation products (IMP) and harmonics of the incoming signals.

Four types of emitters were considered over the frequency band of 5 to 15 GHz with both pulse modulation and CW. The effective radiated power (ERP) in the main lobes is +115 to +120 dBm for pulse emitters and +100 dBm for CW emitters. The sidelobe ERP is +67 to +75 dBm for pulse emitters and +53 dBm for CW emitters. The spurious responses are due to second order intermodulation products ($F_1 + F_2$); second order harmonics ($2F_1$); third order intermodulation products ($2F_1 + F_2$), ($F_1 + 2F_2$); and third harmonic generation ($3F_1$). Receiver saturation was also evaluated. Intermodulation between pulse signals at different frequencies was not considered because of the low probability of occurrence.

The standard four-antenna fine DF (FDF) interferometer used as the basis for the analysis is shown in Figure 4. The approximate capabilities utilizing such a receiver against five selected emitters are shown in Table 1. The spurious responses may be eliminated by several means such as preselection filtering and software computations as indicated in Table 2. The receiver spurious response characteristics can also be significantly improved by providing separate mixers for two frequency bands (diplexing), using high level mixers, and increasing local oscillator power.

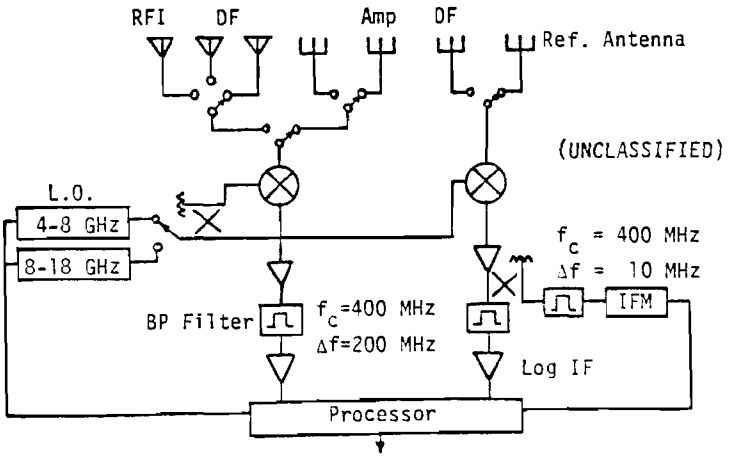

Figure 4. Interferometer block diagram.

TABLE 1. STANDARD RECEIVER CAPABILITY AGAINST SELECTED EMITTERS

Emitter	Sidelobe Detection Range (km)	Receiver Saturation Range (Main Lobe) (km)	Second Harmonic Interference Range (km)	Third Harmonic Interference Range (km)
1	30-33	5.9	59	7.4
2	29-33	3.7	36	--
3	7-9	1.8	--	--
4	18-20	1.3	20	--
5 (CW)	2.5-3	0.4	4.8	--

TABLE 2. METHODS OF ELIMINATING SPURIOUS RESPONSES

Spurious Response	Elimination Technique
Second IMP	Preselector, Calculate $F_1 \pm F_2$
Second Harmonic	Preselector
Third IMP	Calculate $F_1 \pm 2F_2$, $2F_1 \pm F_2$
Third Harmonic	Preselector
Saturation	High Level Mixer, PRI Processing

SECTION 4
FINE DF ERRORS

The generic RFI DF system shown in Figure 4 was formulated and analyzed to determine the processing time line. The salient features of the generic system are (1) angle measurement is performed by an RF interferometer, (2) the necessary receiver sensitivity is provided by a superheterodyne receiver, (3) targets are acquired by performing an initial search over the frequency band of interest, (4) selected high-priority targets are then re-examined and their directions are determined, and (5) target direction is reported to the central processor for further analysis or processing.

The primary error sources for the generic system are:

- o Thermal noise errors,
- o Analog-to-Digital (A/D) converter quantization errors,
- o Rotor blade modulation errors, and
- o Azimuth multipath errors.

Complete compensation is assumed to be provided for system errors (phase match, stability, etc.). The effects of each of the primary error sources on system performance are analyzed below.

The thermal noise errors can be quantified using Equation (6). For a large signal-to-noise (S/N) ratio, the standard deviation of the phase angle error, σ_ϕ, is approximately equal to N/S. For an assumed typical value of S/N of 14 dB and for $D = 10\lambda$, the standard deviation of the spatial error is, from Equation (6), $\sigma_\theta \simeq 0.18°$.

The A/D converter quantization error is reflected into an angle quantization error. A five-bit quantization will result in an angle error of about 0.5° for $D = 10\lambda$. A/D converters having more than five-bit resolution can be used to further reduce angle quantization errors.

The rotor blade modulation error is a periodic error related to the passage of the rotor blade through the field of view of the RF interferometer. The very limited sample of available test data indicate that this modulation produces a pre-processing angular error of about 1° RMS which has a

decorrelation time of 5-20 ms. Sufficient independent samples can be averaged over approximately 100 ms to reduce this error to an acceptable level, i.e., < 0.5°.

The largest expected contribution to fine DF errors is azimuth multipath. When a leading-edge gate is used, the multipath returns come from within an ellipse of constant delay as depicted in Figure 5. Bistatic multipath data were not available for an empirical model, but a limited analytical formulation was deemed useful for gaining insight into the azimuth multipath errors. The analytical formulation was based on the following assumptions:

- o The direct path is a transmitter sidelobe or back lobe.
- o The indirect path is via a bistatic scatterer in the main lobe.
- o The transmitter is scanning the forward sector.
- o The DF system uses leading edge gating.

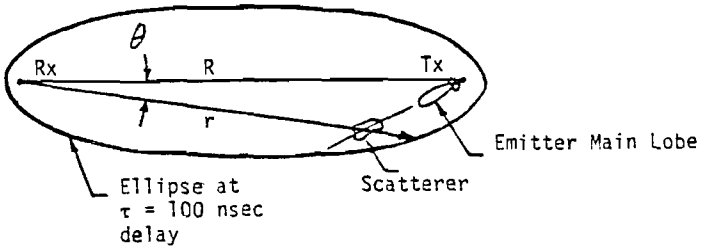

Figure 5. Multipath geometry.

Additional assumptions were: (1) the indirect path power is greater than the direct path power so that the system DFs on the bistatic scatterer, rather than the threat; (2) there are approximately 20 such bistatic scatterers per square kilometer; and (3) the distribution of errors is approximately normal. For an interferometer-to-emitter range of 2 kilometers, assumption (1) requires that the bistatic scattering be at a level of about 15 dBsm.

The probability, $P(\theta)$, that a multipath reflection will occur at a particular angular direction may be computed from

$$P(\theta) = P_e P_i \int_0^r \rho \, d\rho = P_e P_i r^2/2 \qquad (9)$$

where P_e = probability of existence = $20/km^2$

P_i = probability of illumination = 1°/180°.

The assumption for probability of existence that there are 20 bistatic scatterers per square kilometer means that there are 20 natural terrain features, vehicles, or other structures that are oriented such that the emitter main lobe energy reflected to the RFI is large compared to the energy radiated directly to the RFI from the emitter sidelobes. This assumption is highly dependent on the scenario and probably should be considered severe. The assumption for probability of illumination will be valid when the emitter beamwidth is 1° and its main lobe is swept over the ground in a 180° sector that contains the RFI.

For the ellipse of Figure 5, the distance r is a function of the emitter-to-sensor distance, R, the spatial angle, θ, and the difference between the direct and indirect transmission paths, δ. This distance is approximately given by

$$r \approx \frac{1}{1/R + \theta^2/2\delta} . \tag{10}$$

The total RMS angular error is given by

$$\theta_{RMS} = \left[\int_{all\ \theta} P_t(\theta)\theta^2 \, d\theta \right]^{1/2} \tag{11}$$

The total error probability, $P_t(\theta)$, in equation (11) may be considered to consist of two components: one due to multipath errors and one due to all other (noise) errors. Equation (11) may be rewritten to show these components explicitly, i.e.,

$$\theta_{RMS} = \left[(1 - P_m) \int P_n(\theta)\theta^2 \, d\theta + \int P(\theta)\theta^2 \, d\theta\right]^{1/2} \tag{12}$$

where $P_n(\theta)$ = error function without multipath (noise only)

$(1 - P_m)$ = probability that there is no multipath.

The probability that multipath does occur is given by

$$P_m = \int P(\theta) \, d\theta. \tag{13}$$

By combining Equations (9) and (10), we obtain

$$P(\theta) = (P_e P_i)(1/2)\left[\frac{1}{1/R + \theta^2/2\delta}\right]^2 \tag{14}$$

By integrating Equation (14) over the 180° forward sector via Equation (13), we obtain the multipath probability

$$P_m = (P_e P_i)(1.11)(R)(\delta R)^{1/2}. \tag{15}$$

As stated above, the error function without multipath is assumed to be normally distributed so that

$$P_n(\theta) = e^{-a\theta^2}. \tag{16}$$

The second part of Equation (12) is very difficult to integrate using the explicit expansion for $P(\theta)$ given in Equation (14). However, if the distribution of error due to multipath is also normal, a rough approximation to Equation (14) for the case where R = 2 km and δ = 30 m is given by

$$P(\theta) = (P_e P_i)(2e^{-40\theta^2}). \tag{17}$$

For this case, with the noise-only RMS error equal to 0.5°, the total error with multipath included is θ_{RMS} = 1.6°. For R = 4 km and δ = 30 m, the approximate multipath probability function is

$$P(\theta) = (P_e P_i)(2e^{-100\theta^2}) \tag{18}$$

and θ_{RMS} = 1.2° with multipath included.

These predicted azimuth errors are large compared to a desired overall error of 0.5°. Therefore, multipath elimination algorithm processing must be employed. Potential multipath processing includes (1) rejecting 5% of the strongest and 5% of the weakest signals, (2) rejecting 5% of the most erroneous angles before averaging, and (3) averaging as long as possible.

SECTION 5
TIME-LINE ANALYSIS

The analysis of the time required to perform fine DF on multiple emitters is based on the following assumed sequence:

- o Perform an initial frequency search
- o Prioritize targets
- o Examine selected targets
  - Case 1: Sequential examination
  - Case 2
    - Dwell to reduce rotor blade modulation
    - Examine selected targets
    - Revisit until azimuth multipath is acceptable
    - Report target locations
- o Repeat frequency search.

The frequency search time, T_s, is given by

$$T_s = T_1 \Delta/(2B) \tag{19}$$

Where T_1 = dwell time at single frequency,
Δ = RF bandwidth to be searched, and
B = IF bandwidth.

For Case 1 (sequential examination), the fine DF (FDF) time can be computed by

$$\sigma_\theta' = \sigma_\theta/(N_i)^{1/2} = \sigma_\theta/(t_f/\tau_d)^{1/2} \tag{20}$$

$$t_f = \tau_d(\sigma_\theta^2/\sigma_\theta'^2) \tag{21}$$

where σ_θ' = smoothed RMS multipath error,

σ_θ = RMS multipath error,

N_i = number of independent samples,

t_f = time for fine DF, and

τ_d = decorrelation time for azimuth multipath.

For Case 2 (dwell to reduce rotor blade modulation then revisit to reduce multipath), the result is slightly different and depends on the decorrelation times for the various errors. The dwell time is given by

$$\text{Dwell time} = \tau_b \, (\sigma_b^2/\sigma_b'^2) \tag{22}$$

where τ_b = blade modulation decorrelation time,

σ_b = standard deviation of blade modulation errors, and

σ_b' = desired integrated error.

The time to investigate n targets is just n times the dwell time given in Equation (22), i.e., $n\tau_b\sigma_b^2/\sigma_b'^2$. For the case of $n\tau_b\sigma_b^2/\sigma_b'^2 < \tau_d$ (Case 2A), the fine DF time is

$$t_f = \tau_d(\sigma_\theta^2/\sigma_\theta'^2) \text{ (independent of n).} \tag{23}$$

For the converse (Case 2B), where $n\tau_b\sigma_b^2/\sigma_b'^2 > \tau_d$, then the FDF time is

$$t_f = n\tau_b(\sigma_b^2/\sigma_b'^2)(\sigma_\theta^2/\sigma_\theta'^2). \tag{24}$$

The total time line is then the sum of the frequency search time and the fine DF (smoothing) time:

$$\underline{\text{Case 1}}: \quad t = t_1\Delta/(2B) + n\tau_d(\sigma_\theta^2/\sigma_\theta'^2) \tag{25}$$

$$\underline{\text{Case 2A}}: \quad t = t_1\Delta/(2B) + \tau_d(\sigma_\theta^2/\sigma_\theta'^2) \tag{26}$$

$$\underline{\text{Case 2B}}: \quad t = t_1\Delta/(2B) + n\tau_b(\sigma_b^2/\sigma_b'^2)(\sigma_\theta^2/\sigma_\theta'^2) \tag{27}$$

The processing time required to locate multiple emitters to a given accuracy is a strong function of the bistatic multipath decorrelation time τ_d as shown in Figure 6 for the assumed set of basic parameters given in Table 3.

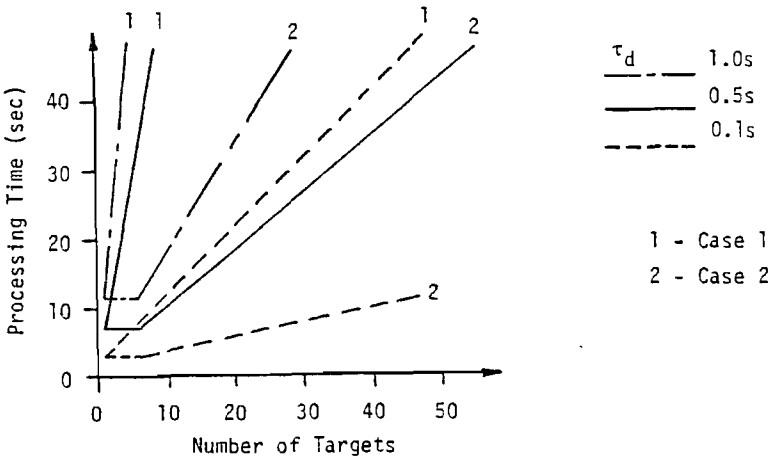

Figure 6. RF Interferometer time-line.

TABLE 3. SYSTEM PARAMETERS FOR THE TIME-LINE ANALYSIS

t_1	= 10 ms (10 pulses)
Δ	= 3.5 GHz
B	= 10 MHz
τ_b	= 10 ms
σ_b	= 1°
σ_θ	= 1.6°
$\sigma'_\theta = \sigma'_b$	= 0.5°

The time-line curves of Figure 6 are based on averaging algorithms only. Other potential multipath processing includes: (1) rejecting some percentages of the strongest and weakest signals and the largest deviation angles, (2) pulse repetition processing and angle gates, (3) phase stability across the pulse, and possibly others. The use of these algorithms prior to averaging may significantly affect the time required to achieve the desired DF accuracy on large numbers of targets. Most or all of these approaches can be

implemented by digital software and/or algorithms in the computer. This may then become a trade-off of computer capacity and complexity against fine DF time. The derivation of the time lines was based upon assumptions relating to the probability of multipath occurrence and the probability of illumination of large bistatic scatterers. These assumptions are strongly sensitive to the scenario and will therefore be highly variable.

SECTION 6
CONCLUSIONS

The capabilities of an RFI sensor mounted above the blades of a helicopter were analyzed to determine the expected performance of such a sensor in a multiple emitter environment. Several different developmental configurations of RFI sensors are available; therefore, a generic sensor configuration was formulated and analyzed. The analysis showed that accurate DF (less than 0.5° RMS spatial error) can be obtained using an RFI sensor. The DF time for a single emitter is quite short and is on the order of 3 to 10 seconds, depending on the assumed value of multipath decorrelation time.

In the case of multiple emitters, preselection filtering may be necessary to reduce spurious responses, and target prioritization will be required to prevent overload of the data processing computer. Multipath and rotor blade modulation elimination algorithms will be necessary to reduce the total DF error to an acceptable level (less than 0.5° RMS). The total time line is a strong function of the multipath decorrelation time, a parameter for which there are little definitive experimental data available. In addition, the derivation of the time-line equations was based on certain assumptions relating to the probability of multipath occurrence and the probability of illumination of large bistatic scatterers. These assumptions are strongly sensitive to the specific scenario and will therefore be highly variable. Additional experimental data are needed to validate or refute these assumptions.